EEET ECOLOGICAL ENGINEERING & ENVIRONMENTAL TECHNOLOGY

Ecological Engineering & Environmental Technology, 2026, 27(6), 354–373
https://doi.org/10.12912/27197050/221679
ISSN 2719–7050, License CC-BY 4.0

Received: 2026.04.17
Accepted: 2026.05.18
Published: 2026.06.01

Comparative optimization of wind turbine power control strategies for improved energy efficiency and load reduction

Atiyah Abdulshfia[1,2*], Aljunayd Aloukili[3], Mohamed Elsakka[4,5], M. Elfaisal Elrefaie[2]

[1] Department of Mechanical Engineering, University of Derna, Derna, Libya
[2] Department of Mechanical Engineering, Al Azhar University, Cairo, Egypt
[3] Renewable Energy Engineering Department, Faculty of Engineering, University of Derna, Derna, Libya
[4] Department of Mechanical Power Engineering, Port Said University, Port Said, Egypt
[5] Faculty of Engineering, East Port Said National University, Salam Misr City, Egypt
* Corresponding author's e-mail: atiyah.abdulshfia@uod.edu.ly

ABSTRACT

The increasing demand for sustainable and resource-efficient energy systems requires wind turbine designs that simultaneously improve energy capture and reduce structural loading during operation. In this study, a Comparative optimization of the NREL Phase VI wind turbine rotor was performed using a genetic algorithm (GA) coupled with blade element momentum (BEM) theory to evaluate the influence of six power control strategies on aerodynamic performance, structural loading, and operational sustainability. The investigated configurations included fixed-speed fixed-pitch, variable-speed fixed-pitch, fixed-speed variable-pitch (pitch-to-stall), variable-speed variable-pitch (pitch-to-stall), fixed-speed variable-pitch (pitch-to-feather), and variable-speed variable-pitch (pitch-to-feather) control systems. Rotor geometry optimization was conducted through simultaneous adjustment of blade chord, twist, and thickness distributions, while turbine performance was evaluated in terms of annual energy production (AEP), thrust, torque, capacity factor, rotor speed, blade pitch angle, and root flap moment. The obtained results demonstrate that pitch-to-feather strategies substantially reduce structural loading while maintaining nearly identical torque output compared to pitch-to-stall configurations. Maximum thrust was reduced by approximately 60%, from 3.72–3.98 kN for pitch-to-stall strategies to 1.55–1.60 kN for pitch-to-feather operation, while torque remained within a narrow range of 1.46–1.49 kN·m for all optimized cases. Variable-speed operation reduced the cut-in wind speed from 4 to 3 m/s and increased the capacity factor from 51.8% to 54.4%. The optimized variable-speed variable-pitch (pitch-to-feather) configuration achieved the highest AEP (52,092 kWh/year) together with the lowest thrust (1.55 kN) and minimum root flap moment (2.27 kN·m), indicating the best balance between energy production and structural load mitigation. In contrast, blade thickness distribution remained nearly unchanged among all control strategies (0.192–0.196 m), indicating that structural constraints dominate thickness optimization. The study is limited to numerical GA–BEM simulations of the NREL Phase VI reference turbine and does not include aeroelastic or full-scale experimental validation. Nevertheless, the obtained findings provide practical guidance for selecting turbine control strategies that improve operational reliability and reduce structural stresses, maintenance demand, and lifecycle loading in wind energy systems. The originality of this work lies in the unified comparative evaluation of six turbine control strategies within a single Comparative optimization framework, with emphasis on the interaction between aerodynamic efficiency and structural load reduction as a pathway toward more sustainable wind turbine operation.

Keywords: wind energy, genetic algorithm, optimization, control methods, horizontal axis, wind turbine.

INTRODUCTION

A significant increase in the proportion of urban dwellers, particularly in developing countries, has led to a marked escalation in global energy demand. Due to the depletion of fossil fuels and escalating environmental concerns, a transition to renewable energy sources is imperative, as it is essential for meeting the rising energy demand while mitigating climate change impacts. Wind energy is currently experiencing unprecedented global growth. As of the end of

2024, the global wind power capacity reached approximately 1.136 GW. China contributed the highest capacity increase at 79.8 GW, followed by the United States, Germany, and India. In 2024, Europe built 16.4 GW, resulting in a total capacity of around 285 GW (Costanzo et al., 2025). For wind energy to contribute effectively to global sustainability goals, turbine designs must go beyond simply maximizing energy capture. Operational reliability, structural load mitigation, material fatigue reduction, and lifecycle efficiency are equally critical. The choice of power control strategy directly influences these sustainability indicators, as it affects the magnitude and frequency of mechanical loads transmitted to critical turbine components, thereby determining maintenance intervals, replacement costs, and the overall carbon footprint of energy generation. Improving the aerodynamic efficiency of energy conversion enables wind turbines to capture more wind energy and enhance energy yield. Using the blade element momentum (BEM) theory and genetic algorithm (GA), Ceyhan et al. (2009) investigated the aerodynamic efficacy of horizontal-axis wind turbine blades. The fitness function was developed utilizing BEM theory, and two design variables, the chord and twist distributions, were tuned to maximize power output. Jureczko et al. In 2005, a GA was developed to enhance the structural stability of wind turbine blades. Aerodynamic forces were determined utilizing blade element momentum theory. Méndez et al. (2006) utilized genetic algorithms alongside BEM theory for aerodynamic optimization of blade chord and twist angle. Hassanzadeh et al. (2016) conducted the aerodynamic shape optimization and analysis of small-scale wind turbine blades using BEM and GA approaches.

Burger and Hartfield (2006) investigated the viability of employing the vortex lattice approach in conjunction with a genetic algorithm to optimize the aerodynamic performance of horizontal-axis wind turbine blades. Clifton-Smith and Wood (2007) employed various evolutionary algorithms to quantitatively optimize tiny wind turbine blades. The objective was to optimize the power coefficient and reduce the initiation duration. The power coefficient was determined using the conventional blade element momentum theory. Chen and Agarwal (2012) utilized a genetic algorithm for the shape optimization of flat-back aerofoils, augmented through integration with an artificial neural network method. Consequently, the operation was markedly expedited. Grasso (2012) concentrated on the aerofoil design at the blade's tip region by numerical optimization. Genetic and gradient-based techniques were employed on a hybrid optimization platform to design a novel family of aerofoils specifically for the root region of the turbine blade, aiming to improve performance and efficiency in energy generation.

Elfarra et al. (2014) utilized computational fluid dynamics, a genetic algorithm, and artificial neural networks to ascertain the optimal cant and twist angles for a winglet on the NREL Phase VI rotor. They accomplished this by modifying the angles at three different wind velocities, yielding a 9% increase in power output. This signifies that genetic algorithms can improve the aerodynamics of wind turbines through optimized blade design. Kaya (2019) employed a support vector regression model, based on CFD solutions, to enhance the spanwise twist distribution of the NREL Phase II and Phase VI rotor blades. This resulted in a 9.2% augmentation in torque for the NREL Phase VI blade and a 131% augmentation for the NREL II blade. These results demonstrate that machine learning-based surrogate models can optimize the aerodynamics of wind turbine blades. Lee and Kwon (2020) employed an artificial neural network and genetic algorithm, combined with CFD-CSD analyses, to optimize the aerodynamic profiles of the NREL Phase VI and NREL 5 MW wind turbine blades, resulting in energy cost reductions of 0.82% and 1.0%, respectively, by modifying blade section contours while considering aeroelastic deformation effects.

Recent advancements in wind turbine technology have underscored the significance of integrating rotor aerodynamic design with power control technologies. Conventional sequential design methodologies that optimize blade geometry without considering the control system frequently fail to attain global optimality due to the intrinsic interdependence between aerodynamic loads and control actions, leading to suboptimal performance and increased operational costs in wind turbine efficiency. As a result of this limitation, control co-design (CCD) methods have emerged as an innovative strategy, enabling the simultaneous optimization of structural and control parameters. Du et al. (2024) developed a comprehensive CCD architecture for floating offshore wind turbines. The results demonstrate that employing a genetic algorithm to optimize chord and twist

distributions, in conjunction with pitch control parameters, yields superior performance compared to conventional sequential methods. This comprehensive perspective emphasizes the necessity of evaluating rotor optimization outcomes across diverse control philosophies rather than treating them as distinct design options.

In addition, the dynamic load reduction capabilities of various control techniques have received considerable attention in current literature. Wang et al. (2024) conducted a comprehensive review of power control approaches for wind turbines, emphasizing that the selection of control strategy substantially influences energy capture efficiency as well as the amplitude and frequency characteristics of structural stresses. Their investigation indicates that pitch-to-feather control consistently outperforms stall-based control in load reduction, particularly at wind speeds exceeding rated levels. Samani et al. (2020) performed a thorough comparative analysis of pitch-to-stall and pitch-to-feather control systems, emphasizing notable differences in aerodynamic load distribution within the pitch actuation system. Their findings indicate that pitch-to-feather control diminishes the angle of attack, consequently reducing thrust and flapwise bending moments. The pitch-to-stall control regulates power by deliberately inducing flow separation, potentially increasing cyclic loads on the blade's structural elements. These concepts provide a theoretical foundation for the different control mechanisms employed in this study.

Papi et al. (2021) performed an extensive case study on small wind turbine design, illustrating that variable-speed pitch-to-feather control can enhance annual energy production by over 12% relative to baseline configurations. Sesalim and Naser (2024) improved the S809 aerofoil segment employed in the NREL Phase VI rotor. They demonstrated that changes in the twist distribution significantly affect the variation of the sectional angle of attack along the blade span.

Despite these substantial contributions, several important gaps remain in the current literature. Most previous studies have investigated either aerodynamic rotor optimization or turbine power control independently, while the combined influence of control strategy on aerodynamic efficiency, structural loading, and operational sustainability has received limited attention. In many cases, optimization studies focus primarily on maximizing energy capture without adequately considering how control-induced load variations affect structural stresses, maintenance demand, and long-term operational reliability of wind energy systems. In addition, although the NREL Phase VI turbine has been extensively investigated, a systematic comparison of multiple power control strategies within a unified Comparative optimization framework remains insufficiently explored. Previous studies rarely evaluated how different control philosophies simultaneously influence blade geometry, aerodynamic performance, and structural loading characteristics. The relationship between control strategy and blade thickness distribution has also not been clarified in previous studies, despite its importance for structurally efficient rotor design.

To address these gaps, the present study integrates genetic algorithm optimization with blade element momentum theory to evaluate six power control strategies for the NREL Phase VI rotor under a unified framework. The study focuses not only on aerodynamic performance and annual energy production, but also on the reduction of structural loads associated with turbine operation. Particular attention is given to the relationship between power regulation strategy, load distribution, and rotor geometric characteristics in order to identify configurations that improve both energy efficiency and operational sustainability.

The aim of this study is to determine the power control strategy that provides the most sustainable balance between annual energy production and structural load reduction for the NREL Phase VI wind turbine rotor using a Comparative GA–BEM optimization framework.

METHODOLOGY

This study employs a theoretical approach using the open-source code HARP_Opt (Horizontal Axis Rotor Performance Optimization), developed by Sale (2010). The code was funded by the U.S. Department of Energy's Marine Hydrokinetic Program at the National Renewable Energy Laboratory (NREL). It utilizes a Comparative evolutionary algorithm in conjunction with a Blade Element Momentum (BEM) flow model to design horizontal-axis rotors for wind and water turbines. The genetic algorithm resolves optimization issues by emulating the mechanisms of biological evolution; it successively alters a population of individuals through genetic alteration

and reproductive laws, thus producing successive generations of "superior" candidate solutions. Figure 1 shows the fundamental idea behind the code. The base code can also be used to configure different rotor control strategies, such as fixed or variable blade pitch settings and fixed or variable rotor speed settings. HARP_Opt can optimize one goal or several at the same time. The main purpose of the optimization is to maximize annual energy production (Sale, 2010). A Rayleigh, Weibull, or other defined flow distribution is used to estimate annual energy production. Maximum power points are monitored while considering system constraints on the allowable power output. Figure 2 shows a screenshot of the graphical user interface (GUI) of HARP_Opt, where the user can enter variables according to the desired optimization objectives and constraints.

The BEM theory employed here is a simplified aerodynamic model; the limitation of this case is that it does not fully capture three-dimensional rotational effects (stall delay), dynamic inflow, or tip losses, particularly under yawed or turbulent conditions.

General description of genetic algorithms

Genetic algorithms (GAs) are stochastic methods that utilize search strategies mimicking natural evolution; hence, their terminology is derived from biological concepts, as summarized in Table1 (Shopova et al., 2006). GAs begin by generating an initial population of candidate solutions (chromosomes), typically initialized randomly within the solution space. The population advances toward enhanced chromosomes by three genetic mechanisms: selection, recombination, and mutation. Selection determines which chromosomes are chosen for reproduction based on their fitness values. Crossover combines the characteristics of two parent chromosomes to produce offspring. Mutation introduces random variations into the offspring with a specified probability. Through the implementation of these three operators, new generations replace parental chromosomes to produce a new generation, perpetuating the cycle until the optimization criterion is met.

The fundamental genetic algorithm, illustrated in Figure 3 (Pasamontes et al., 2014),

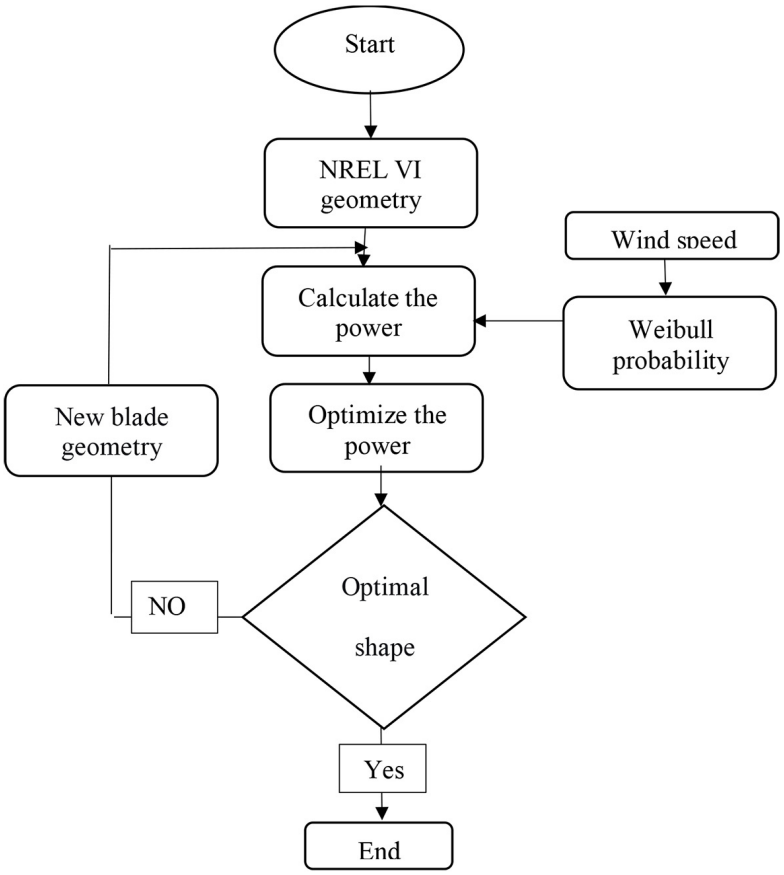

Figure 1. Flowchart of the horizontal axis rotor performance optimization (HARP_Opt) process showing the iterative genetic algorithm loop for blade geometry optimization

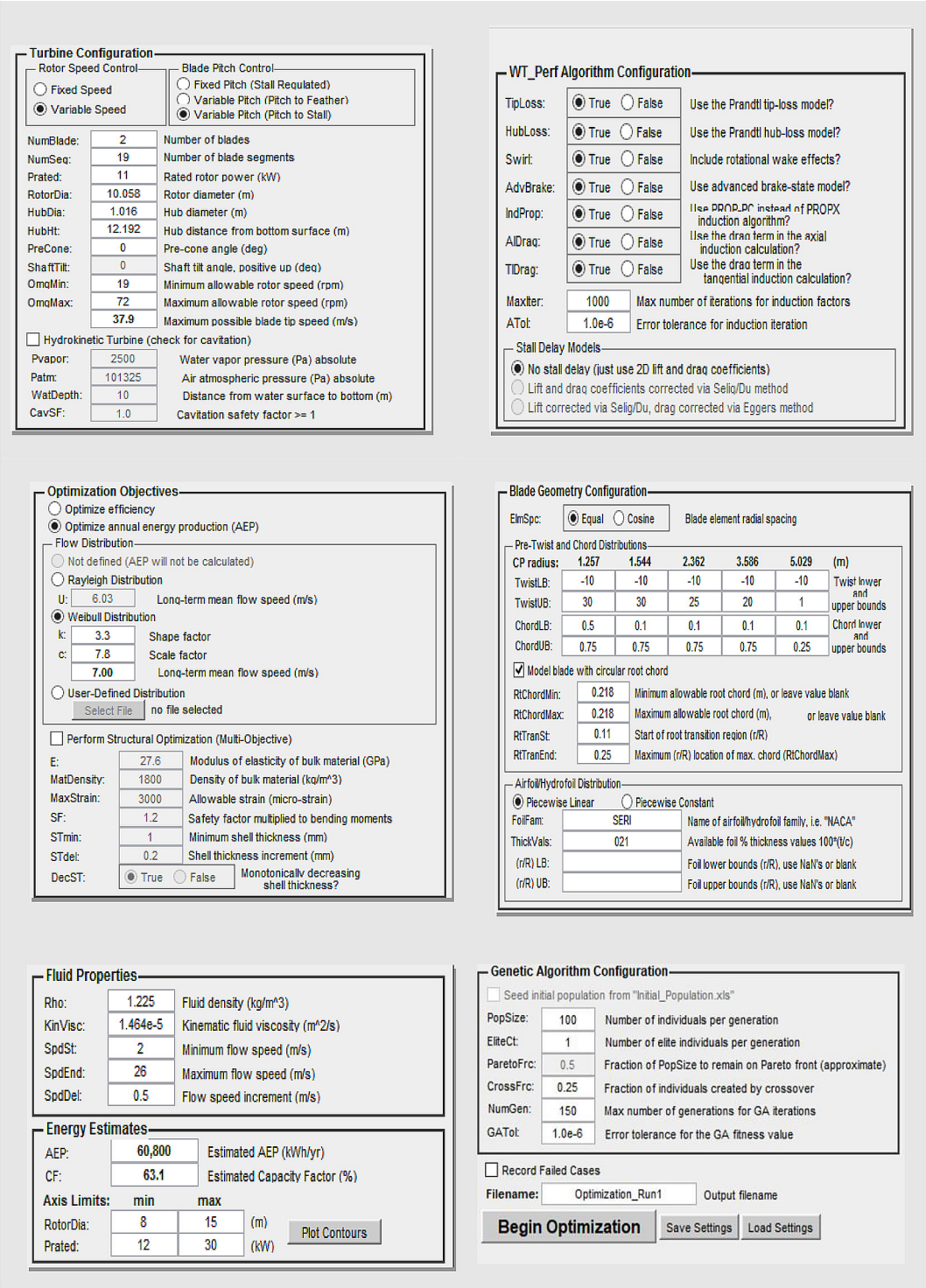

Figure 2. GUI of HARP_OPT with user input variables for wind turbine optimization

functions with a fixed-size population. In the initial generation, BASIC (Shopova et al., 2006), a genetic algorithm designed for engineering optimization problems, produces an entirely random population. The algorithm then computes fitness and objective function values. Reproduction commences with selective bias: fitness values are employed to produce the most advantageous samples for crossover. Randomly picked persons pair to match the amount of samples. Upon meeting a crossover probability, a couple's chromosomes recombine to yield two kids; otherwise, the parents' chromosomes are transmitted to the progeny unaltered. Subsequently, upon reaching a specified mutation probability, every gene on each child chromosome undergoes mutation.

Table 1. Genetic algorithm terminology (Shopova et al., 2006)

Genetic terminology	Mathematical programming equivalent
Generation	Iteration
Chromosome or individual or chromosome genotype	Coded vector of control variables
Chromosome phenotype	Vector of real values of control variables
Gene—part of chromosome which represents given feature	Coded particular variable
Morphogenesis or growth function-transforms chromosome genotype in chromosome phenotype	Decoding function
Population-set of parent chromosomes	Set of vectors of control variables
Objective function	Quality model characteristic for optimization
Fitness function	Normalized objective function at iteration

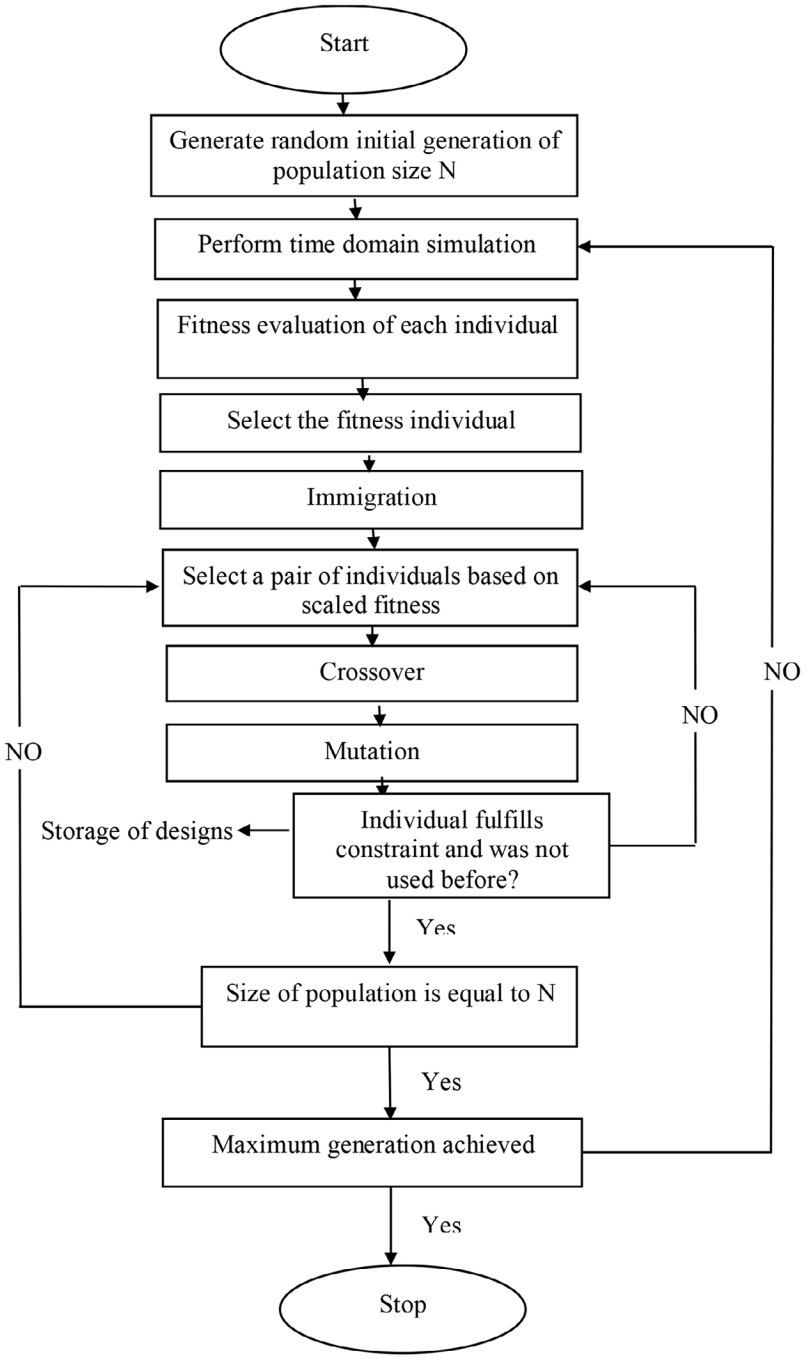

Figure 3. Flow chart of genetic algorithm (Pasamontes et al., 2014)

Ultimately, replacement selection generates the subsequent generation: progenitors and descendants amass in a replacement pool, the optimal individual (overall best solution) is chosen for the new population, and the remaining chromosomes are randomly selected until the new population is fully constituted. The generation counter subsequently increases. BASIC employs the generation number as a criterion for termination (Shopova et al., 2006). If satisfactory, the optimal solution identified is presented as the answer; if not, fitness functions are computed for the new population, and the process reiterates (Mirjalili et al., 2019).

Definition of the turbine

The NREL Phase VI wind turbine is a two-bladed horizontal-axis wind turbine engineered for both axial and yawed flow situations. The turbine underwent extensive testing in the NASA Ames wind tunnel, measuring 24.38 m by 36.57 m, throughout a broad spectrum of operational conditions (Hand, 2001). The NREL Phase VI rotor blade is constructed using S809 aerofoil sections, as depicted in Figure 4. The twist angle and chord length vary along the blade's length, as illustrated in Figure 5. The geometry of the wind turbine (refer to Figure 6) and its operating characteristics are presented in Tables 2 and 3.

Parameter setup of the optimization

It is impractical to define the chord length and pre-twisting angle at multiple locations along the blade span; consequently, the chord length and pre-twist angles were modeled using Bezier curves based on design values at five control points along the blade span, while the percentage thickness was interpolated through Bezier curves derived from design values at three control points. Accordingly, fifteen design factors were evaluated: five pertaining to pre-twisting angles, five related to chord, and five concerning thickness. The initial values for the 15 design variables in genetic algorithms and micro genetic algorithms are indeterminate, as the initial feasible candidate solutions can be generated arbitrarily. Tables 4 and 5 outline the essential parameters for GAs and micro genetic algorithms (micro GAs), encompassing the control points and the minimum and maximum boundary values for chord length and twist angles. In ordinary unconstrained optimization contexts, the mutation probability is typically assigned a low value.

Comparison between the results of GAs and micro gas

Figure 7 illustrates the results of 10 trials obtained using the GA and micro GA for various

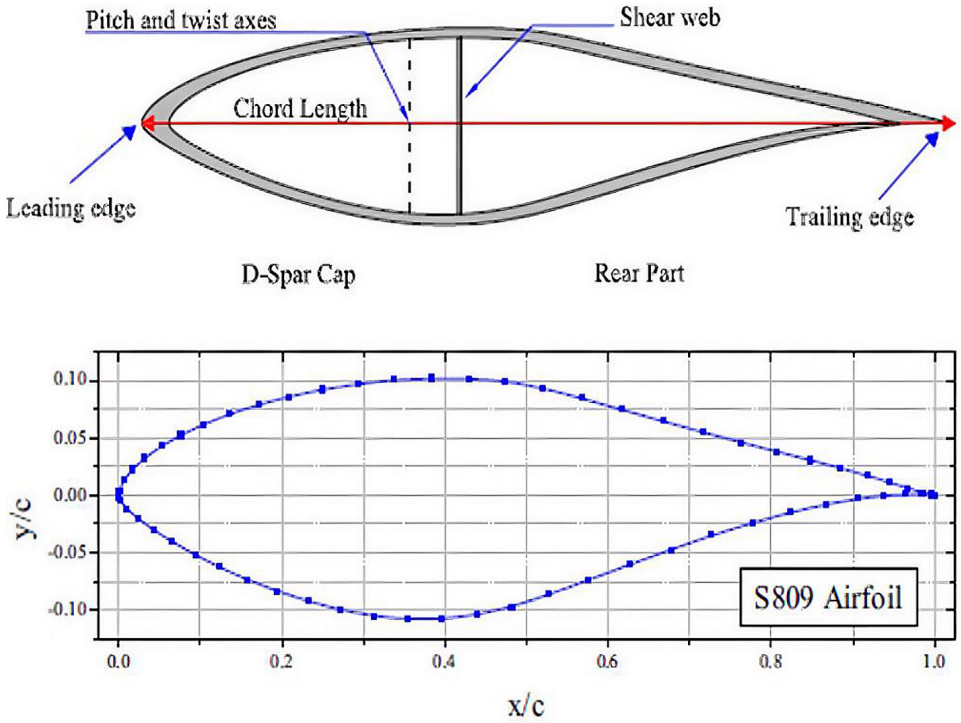

Figure 4. S809 airofoil (Hand, 2001)

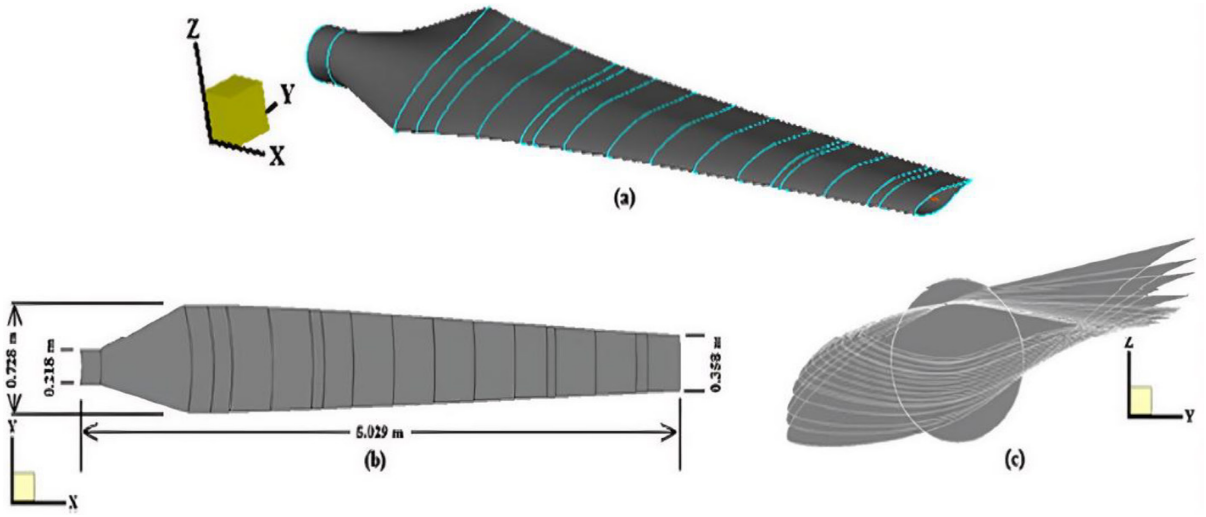

Figure 5. Distributions of the S809 aerofoil sections and the twist angle along the blade (Lee, et al.,2016)

Table 2. Geometry and operating parameters of the turbine (Lee et al., 2016)

Parameters	Value
Number of blades	2
Rotor diameter	10.056 m
Rotational speed	72 rpm
Cut-in wind speed	5 m/s
Rated power	10 kW
Cone angle	0°
Rotor location	Upwind
Power regulation	Stall regulated
Blade tip pitch angle	3°
Blade profile	S809
Blade chord	0.358–0.728 m
Blade thickness (t/c)	21%
Hub diameter	1.016 m
Hub height	12.192 m
Root type	Cylindrical root

Table 3. Chord and twist angle variations along the NREL Phase VI blades (Lee et al., 2016)

Radial distance r (m)	Span station r/R	Chord length (m)	Twist angle (deg)
0.508	0.101	0.218	0
0.660	0.131	0.218	0
1.343	0.267	0. 737	18.074
1.510	0.300	0. 728	14.292
1.648	0.328	0.697	11.909
1.952	0.388	0.666	7.979
2.257	0.449	0.636	5.308
2.343	0.466	0.627	4.715
2.562	0.509	0.605	3.425
2.867	0.570	0.574	2.083
3.172	0.631	0.543	1.150
3.476	0.691	0.512	-0.494
3.781	0.752	0.482	-0.015
4.023	0.800	0.457	-0.381
4.086	0.812	0.451	-0.475
4.391	0.873	0.420	-0.920
4.696	0.934	0.389	-1.352
4.780	0.950	0.381	-1.469
5.029	1.000	0.358	-1.775

blade characteristics. The figure indicates that the results achieved with GA exhibit greater convergence and consistency compared to those obtained with Micro GA. Table 6 displays the mean AEP and coefficient of variation COV for GAs and micro GAs across 10 independent trials. GAs attained a superior mean AEP (51,860.9 kWh) with remarkable consistency (COV = 0.909%), whereas micro GAs produced a lower mean AEP (48,873.3 kWh) with considerably greater variability (COV = 12.41%). The low COV (0.9%) for GA is attributed to the relatively large population size (100) and convergence tolerance (1×10^{-6}), which ensure consistent convergence across independent trials. The higher COV (12.4%) for micro GA reflects its smaller population (10), which reduces genetic diversity and increases variability. These findings indicate that GAs exhibit greater reliability and stability compared to Micro GAs for blade shape optimization, notwithstanding the reduced computing expense associated with Micro GAs.

Figure 6. The NREL phase VI upwind turbine (Hand, 2001)

Table 4. The GA configuration

Genetic algorithms		
Parameters	GAs	Micro GAs
Number of population	100	10
Maximum generation	100	100
Function tolerance	1 × 10-6	1 × 10-6
Crossover probability	0.25	0.25
Mutation probability	Adaptive	Adaptive
Elitism	Yes	Yes

RESULTS AND DISCUSSION

Validation

The validation analysis depicted in Figure 8 juxtaposes the power output predictions from the genetic algorithm (GA) optimization with BEM using HARP_Opt and the BEM theory (using QBlade software) against the experimental NREL Phase VI wind turbine data across a wind speed spectrum of 0 to 25 m/s, illustrating remarkable concordance that substantiates the precision and dependability of the developed optimization code. At wind speeds below 10 m/s, all three datasets show very similar power outputs. The GA and BEM predictions show excellent agreement with the experimental values at 5 m/s (1.8 kW), 7 m/s (3.5 kW), and 10 m/s (7.5 kW). This shows that both computational methods accurately capture the aerodynamic performance when the rotor is operating at optimal tip-speed ratios, which are below-rated conditions. In the above-rated range of 12 to 16 m/s, where the turbine reaches its rated power limit of about 9.5 kW, both the GA and BEM theory predictions continue to match the experimental data closely, with maximum differences of no more than 0.1 kW. When wind speed is 18 m/s or greater, genetic algorithm predictions are within 0.2 kW of experimental values. The rotor's support stall and load shedding behavior are accurately captured by the optimization framework, since the turbine's power output remains consistent between 8.8 and 9.5 kW. The genetic algorithm and blade element momentum curves are nearly comparable across wind speeds. This indicates that the genetic algorithm combined with blade element momentum theory keeps the basic accuracy of aerodynamic modeling while allowing for optimization of blade geometry. The stall region begins at approximately 11 m/s, where the power starts to decrease after its peak at 10 m/s. Deep stall conditions are observed between 15 and 22 m/s, where the experimental power drops to 8.3–9.0 kW. At 18 m/s (deep stall), the GA prediction shows a relative error of 15.57% (7.16 kW GA vs. 8.48 kW experimental), and the BEM prediction shows an error of 8.49% (9.20 kW BEM vs. 8.48 kW experimental). At 22 m/s, the GA prediction is highly accurate, with

Table 6. Comparison between AEPs of GAs, micro GAs

Parameter	Parameters	GAs	Micro GAs
AEPs	Average (kWh)	51860.9	48873.3
	COV (%)	0.909	12.41

Table 5. Control points, lower and upper boundary values for chord and twist angle

Control point (m)		1.534	1.8	2.557	3.691	5.028
Chord length (m)	LBVs	0.1	0.1	0.1	0.1	0.1
	UBVs	0.75	0.75	0.7	0.7	0.25
Twisting angle (deg)	LBVs	-10	-10	-10	-10	-10
	UBVs	30	30	25	20	1

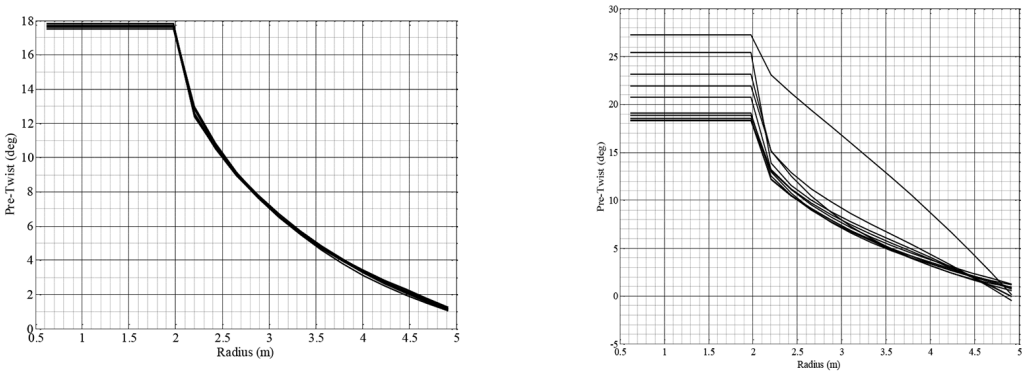

Genetic Algorithms Micro Genetic Algorithms

(a)- PreTwist angle with Radius

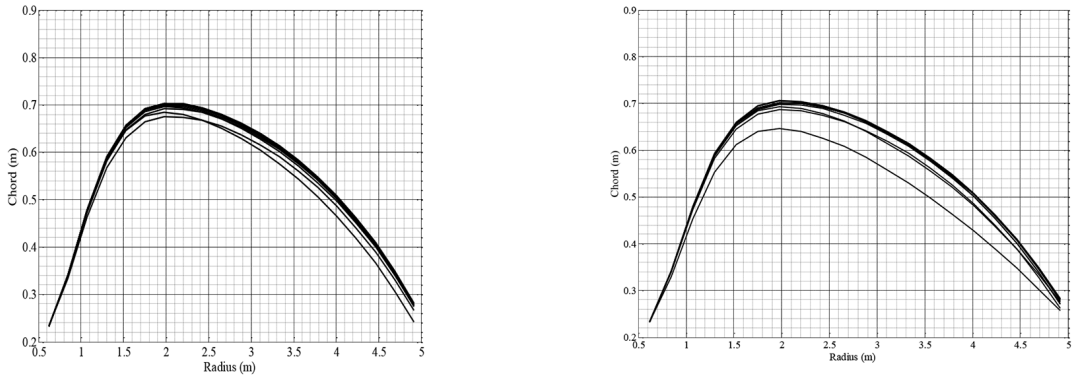

Genetic Algorithms Micro Genetic Algorithms

(b)- Chord with Radius

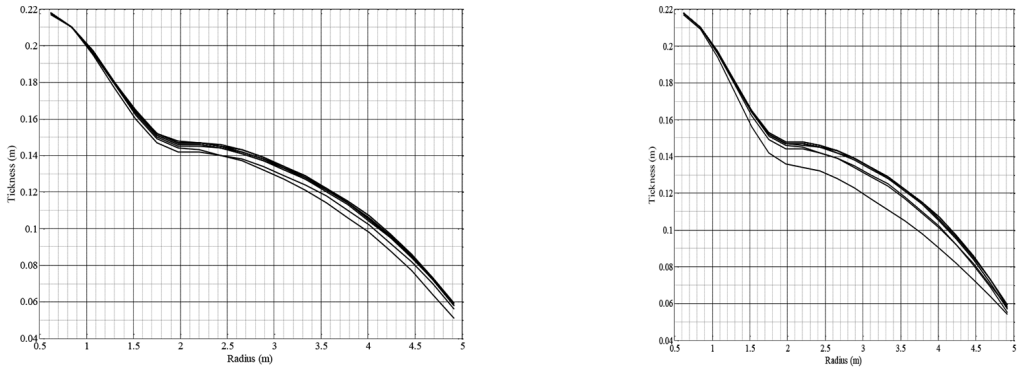

Genetic Algorithms Micro Genetic Algorithms

(c)- Thickness with Radius

Figure 7. Results of 10 trails obtained from genetic algorithm and micro genetic algorithm for different blade parameters

a relative error of only 0.94% (8.23 kW GA vs. 8.31 kW experimental), while the BEM prediction shows a more typical error of 14.11% (9.48 kW BEM vs. 8.31 kW experimental), which lies within the expected 3–15% range for BEM-based predictions under deep stall conditions. This validation application shows that the HARP_Opt code, which uses GA-based optimization with BEM theory, makes predictions that match experimental measurements very well across the full range of operational conditions. This means that it is a strong and reliable way to optimize the geometry of wind turbine rotors for different power control strategies.

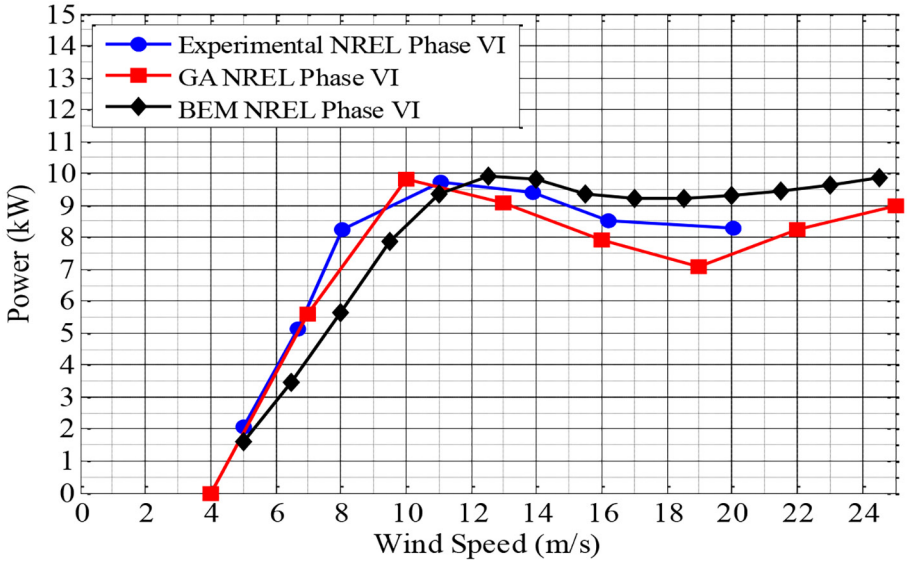

Figure 8. Validation of power output predictions for the NREL phase VI wind turbine – comparison of experimental data (Hand, 2001), BEM theory, and GA-optimized results

Optimization of the NREL phase VI wind turbine rotor using different power controls

Table 7 and Figure 9 present a comprehensive comparison of the chord distributions along the blade of the NREL Phase VI wind turbine. The turbine was optimized through different power control methods, including fixed and variable speed options, as well as fixed and variable pitch configurations, such as pitch-to-feather and pitch to stall. Table 7 shows that the base turbine, which is controlled by stalling, has the largest maximum chord (0.737 m) and the smallest minimum chord of 0.358 m. This analysis indicates that it serves as an effective baseline design. The variable speed and variable pitch control configuration possesses the largest maximum chord 0.734 m, whereas the fixed speed and fixed pitch configuration exhibits the smallest minimum chord 0.246 m. The fixed speed and variable pitch (pitch-to-feather) control yields the minimal chord length 0.674 m, indicating that this approach facilitates the design of a more slender and lightweight blade. Figure 9 illustrates that all control systems exhibit a comparable overall trend: the chord length increases rapidly from the root to approximately mid-span (around 2–3 m radius) and subsequently declines gradually toward the tip. However, significant differences are present; the variable speed – variable pitch (pitch-to-stall) and fixed speed – variable pitch (pitch-to-stall) configurations demonstrate slightly increased chord values in the outboard region, while the fixed speed – variable pitch (pitch-to-feather) configuration consistently shows diminished chord values across the entire blade. Integrating both analyses reveals a distinct correlation: control strategies that produce thinner blades and smaller chords are typically associated with pitch-to-feather configurations, whereas pitch-to-stall strategies correlate with larger chords, particularly in the central span. The fixed speed and variable pitch (pitch-to-feather)

Table 7. The differences in chord distributions optimized under various power control techniques

Control system	Maximum chord (m)	Minimum chord (m)
Fixed speed and variable pitch (pitch-to-feather)	0.674	0.267
Fixed speed and fixed pitch	0.715	0.246
Fixed speed and variable pitch (pitch-to-stall)	0.726	0.263
Variable speed and variable pitch (pitch-to-stall)	0.734	0.271
Variable speed and fixed pitch (stall regulated)	0.723	0.27
Variable speed and variable pitch (pitch-to-feather)	0.694	0.269
Base turbine (stall regulated)	0.737	0.358

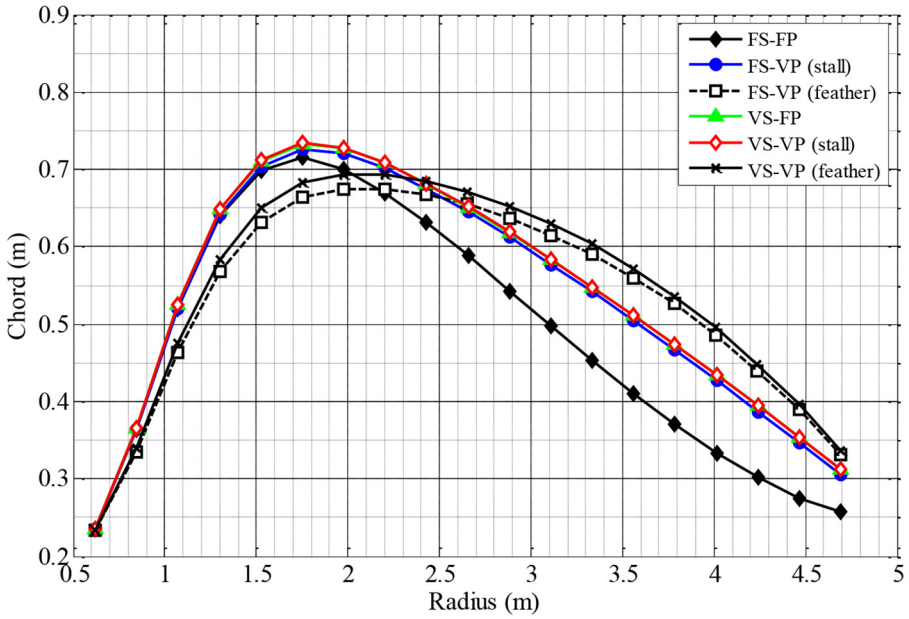

Figure 9. The chord distributions along the blade of NREL phase VI wind turbine utilizing various power control methods

control is noteworthy as it enables the production of the smallest chord, 0.674 m, while maintaining a smooth and aerodynamically efficient chord distribution. This renders it a viable option for producing lightweight and inexpensive blades. The selection of power control methodology significantly influences chord distribution. For instance, pitch-to-feather strategies typically produce blades that are narrower and possess shorter chord lengths, whereas pitch-to-stall strategies tend to result in larger chord distributions, particularly in the mid-span region.

Figure 10 and Table 8 provide a detailed examination of twist angle distributions along the NREL Phase VI wind turbine blade, optimized under different power control methodologies, including fixed and variable speed, as well as fixed and variable pitch configurations (pitch-to-feather and pitch-to-stall). The graphical representation Figure 10 demonstrates that all control systems

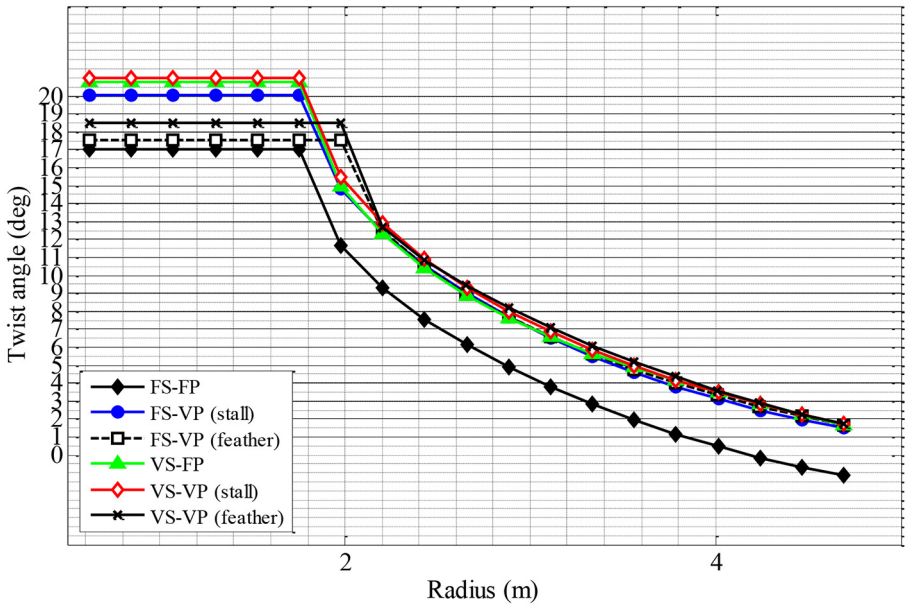

Figure 10. Twist angle distributions along the blade radius of the NREL phase VI rotor under various power control strategies

Table 8. The minimum and maximum twist angles along the NREL phase VI rotor blade utilizing different power control methods

Control system	Maximum twist angle (deg)	Minimum twist angle (deg)
Fixed speed and variable pitch (pitch-to-feather)	17.52	1.11
Fixed speed and fixed pitch	17.05	-1.57
Fixed speed and variable pitch (pitch-to-stall)	20.06	1.013
Variable speed and variable pitch (pitch-to-stall)	20.97	1.23
Variable speed and fixed pitch (stall regulated)	20.75	1.01
Variable speed and variable pitch (pitch-to-feather)	18.47	1.23
Base turbine (stall regulated)	18.074	-1.775

exhibit a similar trend: a rapid reduction in twist angle from the root (≈0.1) to mid-span ($r/R \approx 0.5$), followed by a gradual fall toward the tip ($r/R \approx 1.0$). However, significant discrepancies exist among the configurations in the inboard region. The variable speed and variable pitch (pitch-to-stall) and variable speed and fixed pitch (stall regulated) controls demonstrate the greatest twist angles at the root, surpassing 20°, while the fixed speed and fixed pitch control displays the lowest twist angles in that area. The tabular data Table 8 indicates that the combination of variable speed and variable pitch (pitch-to-stall) control fulfill the highest maximum twist angle of 20.97°, followed by variable speed and fixed pitch at 20.75°, and constant speed with variable pitch (pitch-to-stall) at 20.06°. Conversely, the fixed speed and fixed pitch control yields the lowest maximum twist angle (17.05°) and is the sole design, alongside the base turbine, to attain a negative minimum twist angle (-1.57°), suggesting a risk of aerodynamic instability or blade stall at the tip. The fixed speed and variable pitch (pitch-to-feather) control attains a modest maximum twist angle of 17.52° and a positive minimum twist angle of 1.11°, indicating a well-balanced and aerodynamically efficient twist distribution. By integrating both assessments, a distinct correlation is revealed: pitch-to-stall procedures typically yield elevated twist angles, especially at the root, which may augment aerodynamic torque at low wind velocities but could also elevate structural loads. In contrast, pitch-to-feather procedures yield more mild twist profiles that enhance aerodynamic efficiency and minimize tip losses. The fixed speed and variable pitch (pitch-to-feather) control is notable for achieving a balanced twist distribution without negative angles, positioning it as a potential option for efficient and dependable blade design. The selection of power control methods markedly affects twist angle distribution; pitch-to-stall strategies produce elevated twist angles appropriate for low speed torque generation, whereas pitch-to-feather strategies deliver smoother, more aerodynamically efficient profiles, thereby offering essential perceptions for wind turbine blade optimization.

Figure 11 and Table 9 illustrate the thickness distributions of the NREL phase VI blade across several power control methodologies. Figure 11 illustrates that all control schemes yield essentially indistinguishable thickness profiles: a fast decline from the root to mid-span, succeeded by a steady tapering toward the tip, with all curves exhibiting substantial overlap. Table 9 verifies this consistency, with maximum thickness values fluctuating slightly between 0.192 m and 0.196 m, and minimum thickness values ranging from 0.052 m to 0.057 m across all configurations. In contrast to chord and twist angle distributions, which exhibit significant sensitivity to the power control approach, thickness distribution demonstrates notable insensitivity to the control strategy. This indicates that thickness is predominantly determined by structural necessities: strength and stiffness rather than aerodynamic enhancement. Designers can enhance chord and twist for aerodynamic efficiency without substantively impacting thickness, facilitating independent aerodynamic-structural optimization of wind turbine blades.

Figure 12 and Table 10 illustrate thrust fluctuations for the NREL phase VI rotor across several power control methodologies. Figure 12 illustrates that all techniques swiftly elevate thrust from 0 to 10–12 m/s, subsequently diverging: pitch-to-stall configurations continue to increase, attaining peak thrust levels, whereas pitch-to-feather configurations stabilize or decline, signifying effective load shedding. Table 10 verifies that fixed speed and variable pitch (pitch-to-stall) produces the highest maximum thrust (3.98 kN),

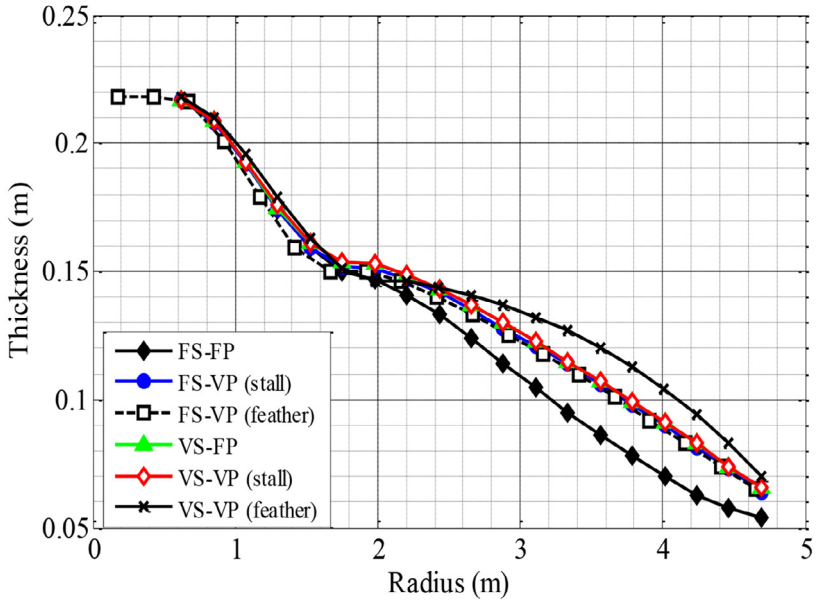

Figure 11. Comparison of NREL phase VI wind turbine thickness distributions along the blade for different power control methods

Table 9. The minimum and maximum thickness along the NREL phase VI rotor blade utilizing different power control methods

Control system	Maximum thickness (m)	Minimum thickness (m)
Fixed speed and variable pitch (pitch-to-feather)	0.195	0.056
Fixed speed and fixed pitch	0.193	0.052
Fixed speed and variable pitch (pitch-to-stall)	0.192	0.055
Variable speed and variable pitch (pitch-to-stall)	0.193	0.057
Variable speed and fixed pitch (stall regulated)	0.193	0.057
Variable speed and variable pitch (pitch-to-feather)	0.196	0.057

whereas variable speed and variable pitch (pitch-to-feather) attains the lowest (1.55 kN), a 60% decrease. Pitch-to-feather strategies mitigate thrust loads during elevated wind speeds, safeguarding structural integrity, while pitch-to-stall strategies optimize energy harvesting but result in increased loads. FS-VP (pitch-to-feather) attains a balanced thrust profile (1.60 kN maximum) with consistent performance, rendering it suitable for load-sensitive applications. Pitch-to-feather strategies offer enhanced structural protection (about 1.6 kN), whereas pitch-to-stall strategies yield greater torque but result in considerably elevated thrust loads (approximately 4.0 kN).

Figure 13 and Table 11 present a thorough examination of torque variations for the NREL phase VI wind turbine rotor, exploring multiple power control strategies, including fixed variable speed and fixed/variable pitch configurations (pitch-to-feather and pitch-to-stall). Figure 13 illustrates that all control approaches present a remarkably similar trend: torque increases rapidly with wind speed from 0 to approximately 8–10 m/s, after which the behavior stabilizes or exhibits a modest plateau across all configurations. In contrast to the thrust behavior seen in Figure 13, where pitch-to-feather and pitch-to-stall strategies significantly diverge at elevated wind speeds, the torque curves for all control approaches remain tightly grouped across the entire wind speed spectrum (0–25 m/s). This indicates that the choice of the power control system has a comparatively minor influence on torque generation, in contrast to its significant effect on thrust loads. The maximum torque values in Table 11 demonstrate notable consistency across all control methods, ranging from (1.29 kN.m to 1.49 kN.m). Variable speed and variable pitch

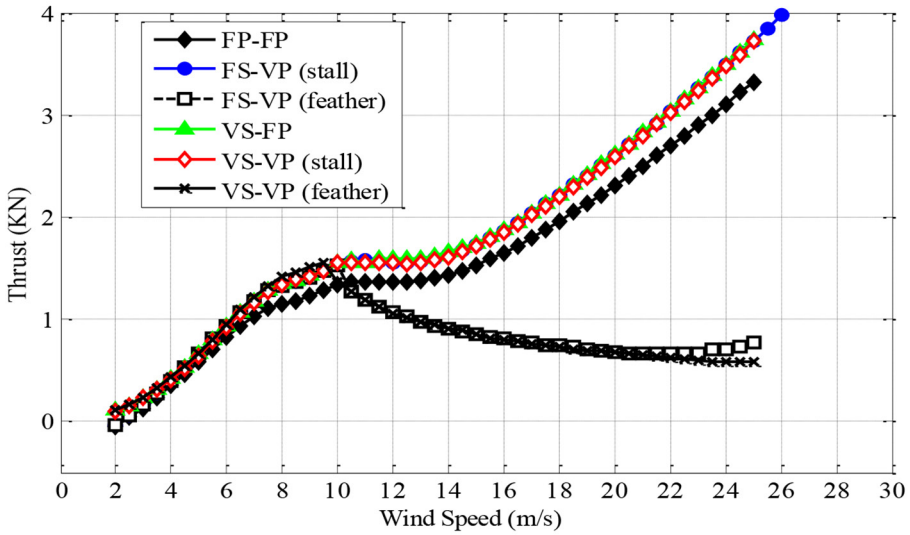

Figure 12. The influences of power control systems on the thrust of the NREL phase VI wind turbine

Table 10. The thrust variation of the NREL phase VI wind turbine rotor under various power control methods

Control system	Maximum thrust (kN)
Fixed speed and variable pitch (pitch-to-feather)	1.60
Fixed speed and fixed pitch (stall regulated)	3.32
Fixed speed and variable pitch (pitch-to-stall)	3.98
Variable speed and variable pitch (pitch-to-stall)	3.72
Variable speed and fixed pitch (stall regulated)	3.74
Variable speed and variable pitch (pitch-to-feather)	1.55

Table 11. The torque variation of the NREL phase VI wind turbine rotor under various power control methods

Control system	Maximum torque (kN.m)
Fixed speed and variable pitch (pitch-to-feather)	1.47
Fixed speed and fixed pitch (stall regulated)	1.29
Fixed speed and variable pitch (pitch-to-stall)	1.46
Variable speed and variable pitch (pitch-to-stall)	1.49
Variable speed and fixed pitch (stall regulated)	1.49
Variable speed and variable pitch (pitch-to-feather)	1.46

(pitch-to-stall) and variable speed and fixed pitch (stall-regulated) controls produce the highest maximum torque of 1.49 kN.m, while the fixed speed - fixed pitch (stall-regulated) control produces the lowest maximum torque of 1.29 kN.m. The pitch-to-feather methods achieve maximum torque values of 1.47 kN.m at a constant speed and 1.46 kN.m at a variable speed. These values are within 1–2% of the peak values attained by pitch-to-stall configurations. The comparable torque performance is a significant observation: pitch-to-feather procedures produce nearly identical torque output to pitch-to-stall strategies while concurrently decreasing thrust loads by approximately 60% (as illustrated in Table 10). A distinctive benefit arises for the regulation of pitch-to-feather. These solutions produce remarkable torque production of 1.46–1.47 kN.m, akin to the ideal pitch-to-stall designs at 1.49 kN.m, while substantially diminishing structural stresses of 1.60 kN in contrast to a maximum thrust of 3.98 kN. Distinguishing between torque and thrust is crucial for wind turbine design, enabling engineers to enhance energy extraction while significantly reducing fatigue damage and structural support requirements. The fixed speed – variable

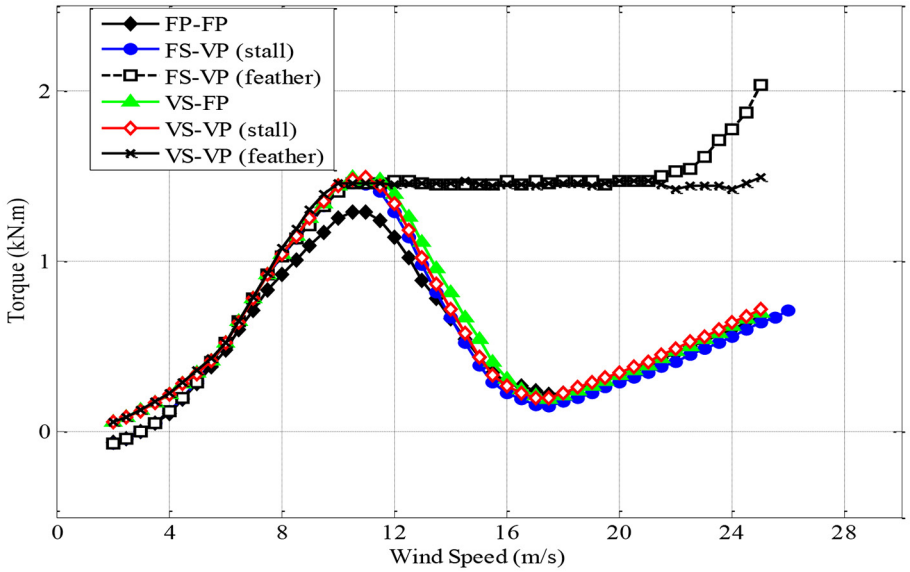

Figure 13. The torque variation of the NREL phase VI wind turbine rotor under various power control methods

pitch (pitch-to-feather) control is illustrious by its capability to produce a high torque of 1.47 kN.m while providing the second-lowest thrust of 1.60 kN, so ensuring an balance between aerodynamic efficiency and structural integrity. In contrast to thrust characteristics, which exhibit significant sensitivity to the control methodology, torque generation is consistently uniform across all power control techniques, with all strategies attaining maximum torque within the range of 1.29–1.49 kN.m. Pitch-to-feather systems excel by producing equivalent torque while significantly enhancing structural protection through the reduction of thrust loads, making them the optimal choice for load-sensitive wind turbine applications.

Figure 14 illustrates the fluctuations in rotor speed and blade pitch angle as functions of wind speed for six power control strategies employed on the NREL Phase VI wind turbine, providing critical information about the responsiveness of each control system to increasing wind speeds for power regulation and structural safeguarding. In the fixed speed - fixed pitch (stall regulated) mode (Figure 14a), the rotor speed remains constant at 72 rpm regardless of fluctuating wind speeds, with the blade pitch angle maintained at zero degrees. This structure relies solely on aerodynamic stall to limit power, hence the moderate thrust 3.32 kN and diminished torque 1.29 kN.m shown in previous analyses. In the variable speed and fixed pitch (stall-regulated) configuration (Figure 14b), the rotor speed incrementally increases from approximately 42 rpm at cut-in to 72 rpm at rated wind speed (around 12–14 m/s), after which it stabilizes, while the blade pitch angle remains constant at zero degrees; this active speed regulation optimizes energy capture in low-wind conditions, yielding elevated torque 1.49 kN.m and substantial thrust (3.74 kN). The variable speed – variable pitch (pitch-to-feather) configuration (Figure 14c) demonstrates the most sophisticated response: rotor speed increases consistently with wind speed up to approximately 15 m/s, reaching around 72 rpm, then progressively decreases at higher wind speeds to alleviate aerodynamic loading, while the blade pitch angle remains at zero until about 12 m/s, after which it positively increases (feathers) to approximately 4–5 degrees at 25 m/s. The feathering motion decreases the angle of attack and lift, clarifying the notably diminished thrust 1.55 kN while maintaining remarkable torque 1.46 kN.m. The fixed-speed and variable-pitch (pitch-to-stall) configuration (Figure 14d) sustains a constant rotor speed of approximately 72 rpm, with the blade pitch angle remaining near zero until approximately 10 m/s, after which it declines to about -4 degrees at 25 m/s; this deliberate negative pitching induces stall, yielding high drag and peak thrust 3.98 kN alongside moderate torque of 1.46 kN.m.

The variable-speed and variable-pitch configuration (Figure 14e) combines speeds ranging from 45 to 72 rpm with negative pitch angles of around -3 degrees, yielding a maximum torque of 1.49 kN.m and significant thrust of 3.72 kN. The fixed-speed and variable-pitch (pitch-to-feather)

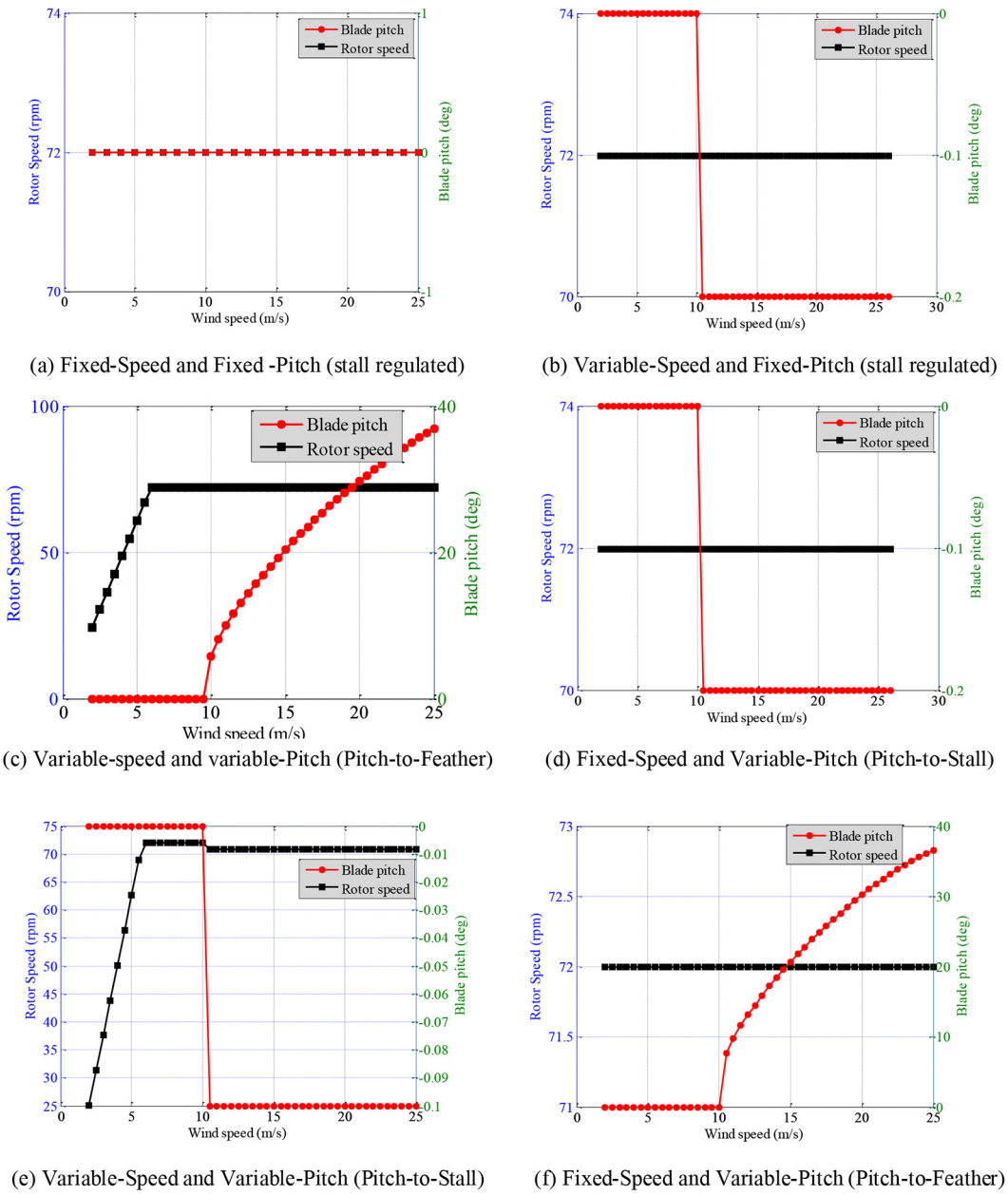

(a) Fixed-Speed and Fixed -Pitch (stall regulated)

(b) Variable-Speed and Fixed-Pitch (stall regulated)

(c) Variable-speed and variable-Pitch (Pitch-to-Feather)

(d) Fixed-Speed and Variable-Pitch (Pitch-to-Stall)

(e) Variable-Speed and Variable-Pitch (Pitch-to-Stall)

(f) Fixed-Speed and Variable-Pitch (Pitch-to-Feather)

Figure 14. The variation in rotor speed and blade pitch angle versus wind speed for various control systems

arrangement (Figure 14f) maintains a constant rotor speed of 72 rpm while gradually increasing the pitch angle to approximately 3–4 degrees, yielding a low thrust of 1.60 kN and notable torque of 1.47 kN.m. Upon integrating all configurations, a clear distinction emerges: pitch-to-feather strategies (Figures 14c and 14f) enhance pitch angle, thereby decreasing angle of attack and lift, which significantly reduces thrust while maintaining torque; in contrast, pitch-to-stall strategies (Figures 14d and 14e) increase pitch angle, leading to a drag-intensive stall that limits power but imposes considerably higher thrust loads. Variable-speed operation (Figures 14b, 14c, 14e) optimizes energy collection in low-wind conditions by allowing rotor speed to increase with wind velocity, whereas fixed-speed operation (Figures 14a, 14d, 14f) is simpler and more cost-effective but demonstrates diminished efficiency at low wind speeds. The variable speed- variable pitch (pitch-to-feather) configuration (Figure 14c) offers the most balanced solution: variable speed optimizes energy capture in low-wind scenarios, while positive pitch feathering protects the turbine in high winds with negligible thrust penalties, yielding the lowest thrust 1.55 kN and near-maximum torque 1.46 kN.m. This arrangement represents a promising solution for modern wind turbine

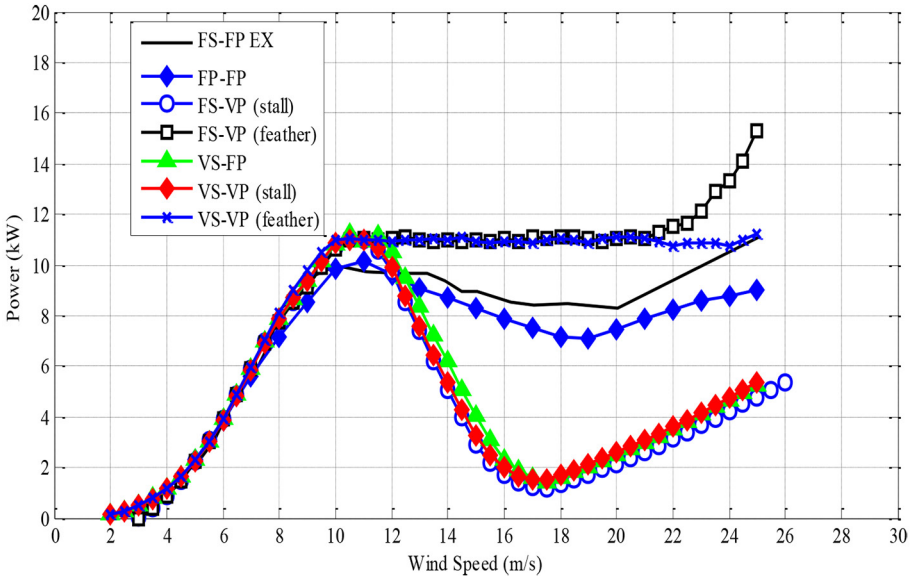

Figure 15. The influence of various power control methods on the power curve of the optimized NREL phase VI wind turbine rotor

control systems, where energy capture and structural integrity are critical.

Figure 15 and Table 12 provide a comprehensive performance comparison of five power control strategies: FS-VP-F (fixed-speed variable-pitch feather), VS-FP (variable-speed fixed-pitch), FS-VP-S (fixed-speed variable-pitch stall), VS-VP-F (variable-speed variable-pitch feather), and VS-VP-S (variable-speed variable-pitch stall) for the optimized NREL phase VI wind turbine rotor. Figure 15 illustrates the power curves, showing that all solutions exhibit the characteristic three-region behavior: a rapid increase in power from cut-in to rated wind speed, constant power at rated conditions, and stable or slightly diminishing power beyond rated speed. Marked disparities exist in cut-in and rated speeds: VS-FP, VS-VP-F, and VS-VP-S achieve lower cut-in speeds of 3 m/s compared to FS-VP-F and FS-VP-S 4 m/s, suggesting that variable-speed operation enhances power capture at diminished wind velocities. This advantage is clearly reflected in the capacity factors (Table 12), where VS-VP-F achieves the highest value at 54.4%, followed by FS-VP-F (53.3%), VS-FP (52.9%), VS-VP-S (52.7%), and FS-VP-S (51.8%). Regarding the maximum power coefficient (Cp max), all strategies demonstrate remarkably similar values (0.371–0.383), indicating that the optimization process successfully improved aerodynamic efficiency regardless of the control method, with FS-VP-F attaining the highest Cp max (0.383). Regarding annual energy production (AEP), VS-VP-F achieves the highest AEP at 52,092 kWh/yr, followed by FS-VP-F at 51,323 kWh/yr, VS-FP at 51,006 kWh/yr, VS-VP-S at 50,590 kWh/yr, and FS-VP-S at 49,942 kWh/yr. This confirms that pitch-to-feather strategies (FS-VP-F and VS-VP-F) exceed pitch-to-stall and fixed-pitch strategies in annual energy capture, with VS-VP-F exhibiting a 4.3% improvement over FS-VP-S. From a structural loading perspective (max root flap moment and max thrust), the two feathering techniques (FS-VP-F and VS-VP-F) demonstrate markedly diminished loads

Table 12. Summary of performance data

Control method	Cut-in speed m/s	Rated speed m/s	Cp max(-)	Capacity factor (%)	AEP kW.hr/yr	Max root flap kN.m	Max torque kN.m	Max thrust kN
FS-VP-F	4	10.5	0.383	53.3%	51323	2.34	1.47	1.60
VS-FP	3	10	0.377	52.9%	51006	4.63	1.49	3.74
FS-VP-S	4	10.5	0.379	51.8%	49942	4.89	1.46	3.98
VS-VP-F	3	10	0.376	54.4%	52092	2.27	1.46	1.55
VS-VP-S	3	10	0.371	52%	50590	4.59	1.49	3.72

compared to all other configurations. VS-VP-F achieves a minimal root flap moment of 2.27 kN.m and a thrust of 1.55 kN, whereas FS-VP-F registers similar low values of 2.34 kN.m and 1.60 kN. In contrast, FS-VP-S exhibits the highest root flap moment 4.89 kN.m and maximum thrust 3.98 kN, indicating an increase of approximately 115% in root flap moment and 157% in thrust relative to VS-VP-F. VS-FP and VS-VP-S demonstrate intermediate but notably increased loads, with a root flap moment ranging from 4.59 to 4.63 kN.m and thrust fluctuating between 3.72 and 3.74 KN. This configuration achieves the highest capacity factor 54.4%, maximum annual energy production (52,092 kWh/yr), minimal root flap moment 2.27 kN.m, and lowest thrust (1.55 kN), demonstrating the optimal balance between energy capture and structural integrity. The combination of variable-speed operation, enabling a low cut-in speed and improved low-wind energy capture, combined with positive pitch feathering for effective high-wind load management, establishes VS-VP-F as the most effective configuration among all control systems. FS-VP-F offers a cost-effective solution with a notably diminished AEP (1.5% lower) and a marginal rise in loads (3% greater thrust), incorporating a simple fixed-speed drivetrain. VS-VP-F appears most promising for utility-scale turbines when improvements in AEP and decreases in structural loads justify the added complexity, while FS-VP-F is an appropriate alternative for smaller or cost-sensitive applications.

CONCLUSIONS

This study demonstrates that the selection of power control strategy in wind turbine operation has a direct influence not only on aerodynamic performance but also on the structural loading regime, which is a key determinant of material demand, service life, and overall system sustainability. A principal outcome of this work is the identification of a consistent load–performance trade-off governed by control strategy. While energy conversion efficiency remains nearly invariant across optimized configurations, significant differences are observed in structural loading, particularly thrust and root bending moments. This indicates that control strategy selection primarily affects mechanical stress distribution rather than energy yield. The results further show that pitch-to-feather operation substantially reduces aerodynamic loading (by up to ~60%) without compromising annual energy production. From an engineering sustainability perspective, this reduction implies lower fatigue accumulation, reduced material stress, and potentially extended operational lifetime of rotor components, which are critical factors in reducing lifecycle environmental impact of wind energy systems. It is also demonstrated that blade geometric thickness is largely independent of control strategy, confirming that structural integrity requirements dominate this parameter. In contrast, aerodynamic shaping parameters (chord and twist) are more responsive to operational control modes, highlighting the importance of integrated aerodynamic–structural–control co-design for resource-efficient turbine systems. Among all investigated configurations, variable-speed variable-pitch pitch-to-feather control provides the most favorable balance between energy production and structural loading minimization. This configuration supports improved operational stability and reduced mechanical stress, which can translate into lower maintenance demand and improved sustainability performance of wind energy systems. Overall, the study contributes to ecological engineering practice by demonstrating that appropriate selection of turbine control strategy can enhance system sustainability not through increased energy capture, but through significant reduction of structural loads and associated material and maintenance requirements. These findings support the development of more resource-efficient and environmentally robust wind energy technologies

REFERENCES

1. Bárcena Pasamontes, L., Gómez Torres, F., Zwick, D., Schafhirt, S., Muskulus, M. (2014). Support structure optimization for offshore wind turbines with a genetic algorithm. In *International Conference on Offshore Mechanics and Arctic Engineering 9*, p. V09BT09A033. American Society of Mechanical Engineers.
2. Burger, C., Hartfield, R. (2006). Wind turbine airfoil performance optimization using the vortex lattice method and a genetic algorithm. In 4th International Energy Conversion Engineering Conference and Exhibit (IECEC) (p. 4051).
3. Ceyhan, Ö., Sezer Uzol, N., Tuncer, İ. H. (2009). Optimization of horizontal axis wind turbines by using BEM theory and genetic algorithm.
4. Chen, X., Agarwal, R. (2012). Optimization of flatback airfoils for wind-turbine blades using a genetic

algorithm. *Journal of Aircraft, 49*(2), 622–629.

5. Clifton-Smith, M., Wood, D. (2007). Further dual purpose evolutionary optimization of small wind turbine blades. In *Journal of Physics: Conference Series 75*, 012017. IOP Publishing.
6. Costanzo, G., Brindley, G., Tardieu, P. (2025*). Wind energy in Europe: 2024 statistics and the outlook for 2025–2030*. Wind Europe.
7. Du, X., Liang, J., Muro, J. L., Qian, G., Burlion, L., Bilgen, O. (2024). Development of a control co-design optimization framework with aeroelastic-control coupling for floating offshore wind turbines. *Applied Energy, 372*, 123728.
8. Elfarra, M. A., Sezer-Uzol, N., Akmandor, I. S. (2014). NREL VI rotor blade: Numerical investigation and winglet design and optimization using CFD. *Wind Energy, 17*(4), 605–626.
9. Grasso, F. (2012). Hybrid optimization for wind turbine thick airfoils. In *53rd AIAA/ASME/ASCE/AHS/ASC Structures, *Structural Dynamics and Materials Conference** (p. 1354).
10. Hand, M. M., Simms, D. A., Fingersh, L. J., Jager, D. W., Cotrell, J. R., Schreck, S., Larwood, S. M. (2001). *Unsteady aerodynamics experiment phase VI: Wind tunnel test configurations and available data campaigns (Report No. NREL/TP-500-29955)*. National Renewable Energy Laboratory.
11. Jureczko, M., Pawlak, M., Mężyk, A. (2005). Optimisation of wind turbine blades. *Journal of Materials Processing Technology, 167*(2–3), 463–471.
12. Kaya, M. (2019). A CFD based application of support vector regression to determine the optimum smooth twist for wind turbine blades. *Sustainability, 11*(16), 4502.
13. Lee, H. M., Kwon, O. J. (2020). Performance improvement of horizontal axis wind turbines by aerodynamic shape optimization including aeroelastic deformation. *Renewable Energy, 147*, 2128–2140.
14. Lee, K., Huque, Z., Kommalapati, R., Han, S. E. (2016). Evaluation of equivalent structural properties of NREL phase VI wind turbine blade. *Renewable Energy, 86*, 796–818.
15. Méndez, J., Greiner, D. (2006). Wind blade chord and twist angle optimization using genetic algorithms. In *Fifth International Conference on Engineering Computational Technology* (pp. 12–15). Las Palmas de Gran Canaria, Spain.
16. Mirjalili, S., Song Dong, J., Sadiq, A. S., Faris, H. (2019). *Genetic algorithm: Theory, literature review, and application in image reconstruction.* In S. Mirjalili, J. Song Dong, & A. S. Sadiq (Eds.), Nature-inspired optimizers: Theories, literature reviews and applications (pp. 69–85). Springer.
17. Papi, F., Nocentini, A., Ferrara, G., Bianchini, A. (2021). On the use of modern engineering codes for designing a small wind turbine: An annotated case study. *Energies, 14*(4), 1013.
18. Pourrajabian, A., Afshar, P. A. N., Ahmadizadeh, M., Wood, D. (2016). Aero-structural design and optimization of a small wind turbine blade. *Renewable Energy, 87*, 837–848.
19. Sale, D. C. (2010). *HARP_Opt user's guide.* NWTC Design Codes.
20. Samani, A. E., De Kooning, J. D., Kayedpour, N., Singh, N., Vandevelde, L. (2020). The impact of pitch-to-stall and pitch-to-feather control on the structural loads and the pitch mechanism of a wind turbine. *Energies, 13*(17), 4503.
21. Shopova, E. G., Vaklieva-Bancheva, N. G. (2006). BASIC—A genetic algorithm for engineering problems solution. *Computers & Chemical Engineering, 30*(8), 1293–1309.
22. Wang, J., Golnary, F., Li, S., Weerasuriya, A. U., Tse, K. T. (2024). A review on power control of wind turbines with the perspective of dynamic load mitigation. *Ocean Engineering, 311*, 118806.